Chalinasterol attenuates ethanol-induced hepatic lipid accumulation by activating β-oxidation

JI HYE KIM[1], MIN YOUNG KIM[1], SEJONG OH[2] and DONG HUN LEE[1]

[1]Department of Biological Sciences, Chonnam National University, Gwangju 61186, Republic of Korea;
[2]Division of Animal Science, Chonnam National University, Gwangju 61186, Republic of Korea

Received August 29, 2025; Accepted February 18, 2026

DOI: 10.3892/br.2026.2130

Abstract. Alcoholic liver disease is a global health burden and, during its earliest stage, alcoholic steatosis, it is still reversible. Ethanol promotes hepatic lipid accumulation by enhancing lipogenesis and suppressing fatty acid oxidation. The present study investigated whether chalinasterol (CA), a natural compound derived from the seaweed *Capsosiphon fulvescens*, can attenuate ethanol-induced hepatic steatosis using *in vitro* hepatocytes and an *in vivo* mouse model. This revealed that CA significantly reduced ethanol-induced lipid accumulation. While it did not change the expression levels of lipogenesis-related genes or reduce reactive oxygen species levels, suggesting that its protective effect was not mediated through these pathways, it upregulated β-oxidation gene expression and increased phosphorylated AMP-activated protein kinase (AMPK) protein levels. It also reduced ethanol-induced elevated serum alanine transaminase and aspartate transaminase levels, indicating that CA attenuated early liver injury. Therefore, CA alleviated ethanol-induced hepatic steatosis by enhancing fatty acid oxidation through AMPK-peroxisome proliferator-activated receptor alpha activation, highlighting its potential as a preventive intervention for early-stage ALD.

Correspondence to: Professor Dong Hun Lee, Department of Biological Sciences, Chonnam National University, 77 Yongbong-ro, Buk-gu, Gwangju 61186, Republic of Korea
E-mail: dhun@jnu.ac.kr

Abbreviations: AICAR, 5-aminoimidazole-4-carboxamide-1-β-D-ribofuranoside; ALD, alcohol-related liver disease; ALT, alanine transaminase; AMPK, AMP-activated protein kinase; AST, aspartate transaminase; CA, Chalinasterol; CPT1A, carnitine palmitoyltransferase 1A; DMEM, Dulbecco's modified Eagle medium; DMSO, dimethyl sulfoxide; EtOH, ethanol; FASN, fatty acid synthase; H_2O_2, hydrogen peroxide; H&E, hematoxylin & eosin; LDC, Lieber-DeCarli; MDA, malondialdehyde; PBS, phosphate-buffered saline; PPARα, peroxisome proliferator-activated receptor α; ROS, reactive oxygen species; SCD1, stearoyl-CoA desaturase 1; SREBP-1, sterol regulatory element-binding protein 1; TG, triglyceride

Key words: chalinasterol, ethanol, steatosis, β-oxidation, alcoholic liver disease

Introduction

According to the World Health Organization, approximately 43% of adults worldwide drink alcohol, and 3 million people died from alcohol consumption-related causes in 2016 (1). Alcohol is a major global health risk factor and is considered to be the cause of many diseases, including cardiovascular disease, diabetes, cancer, and liver disease (2). Alcohol-related liver disease (ALD) is a spectrum of disorders that include alcoholic steatosis, steatohepatitis, fibrosis, and cirrhosis (3). Since the late-ALD stage liver damage associated with cirrhosis cannot be repaired, requiring liver transplantation (4), steatosis treatment should be administered in the early stage of ALD.

Hepatic steatosis is an early symptom seen in alcohol-related conditions, and it occurs in more than 90% of binge drinkers (5). Alcoholic fatty liver is characterized by the accumulation of fat in hepatocytes (5). Ethanol (EtOH) induces lipid accumulation by inducing the synthesis of fatty acids in the liver or reducing fatty acid oxidation (6). Additionally, it promotes triglyceride accumulation in liver through lipogenesis, leading to alcoholic steatosis (7). Fatty acids are synthesized by fat-producing enzymes, including fatty acid synthase (FASN) and stearoyl-CoA desaturase 1 (SCD1), which are regulated by the transcription factor sterol regulatory element-binding protein 1 (SREBP-1) (8). Ethanol induces SREBP-1 cleavage increasing SREBP-1c production, and activated SREBP-1c induces the expression of lipogenic enzymes that enhance fatty acid synthesis in the liver (9). Fatty acids produced in the liver are broken down via β-oxidation; however, EtOH interferes with this process (9). Once activated, peroxisome proliferator-activated receptor alpha (PPARα) enhances the expression of proteins involved in fatty acid oxidation, but EtOH reduces the expression of PPARα, inhibiting fatty acid oxidation, and thus, fat accumulates in the liver (10). Inhibiting EtOH-induced increases in lipid synthesis or decreases in fatty acid oxidation is a promising treatment strategy for EtOH-induced hepatic steatosis.

Recent studies have shown that physiologically active compounds derived from natural resources, such as seaweed, can regulate metabolic pathways and alleviate liver damage (11,12). Seaweed contains compounds with a variety

of effects, such as antioxidant (13), anti-inflammation (14), and anti-obesity (15) activities; therefore, it is widely used in metabolic disease research. One of the most consumed seaweed species in Korea is *Capsosiphon fulvescens*. Previous studies have shown that *C. fulvescens* affects lipid metabolism and obesity (12,16). Islam *et al* (17) investigated the association between three compounds separated from *C. fulvescens* by EtOH extraction, along with an aldose reductase inhibitor related to diabetes. Chalinasterol (CA; 24-methylenecholesterol), one of the three extracted compounds, showed potential as an aldose reductase inhibitor but was less effective than the other two. However, the pharmacological functions of CA beyond aldose reductase inhibition remain unclear, and its effects on hepatic lipid metabolism have not been investigated. Thus, this study aimed to determine whether CA attenuates EtOH-induced lipid accumulation in the liver and investigate the mechanisms underlying its effects in cell and mouse models.

Materials and methods

Cell cultures and treatments. Mouse hepatocyte cell line AML12 was cultured in Dulbecco's modified Eagle's medium (DMEM)/F-12 nutrient mixture medium. Human hepatocyte cell line Huh7 was cultured in DMEM containing 15 mM HEPES, L-glutamine, sodium bicarbonate. Both media were supplemented with fetal bovine serum at 10% and penicillin/streptomycin at 1%, and all cultures were kept at 37˚C in a humidified incubator with 5% CO_2. To establish early-stage alcoholic liver injury (steatosis) *in vitro*, both AML12 and Huh7 cells were treated with 100 mM EtOH, a well-established concentration for inducing intracellular lipid accumulation without causing excessive cell death, for 24 h with or without a 12 h pre-treatment with 4 μM CA. To minimize the effects of EtOH evaporation and ensure consistent exposure, the culture medium was replaced with fresh medium containing 100 mM EtOH every 12 h. The CA was purchased from MedChemExpress (Monmouth Junction, USA) and dissolved in dimethyl sulfoxide (DMSO) to prepare a stock solution, which was then diluted in the culture medium to a final concentration of 4 μM. As a positive control for AMP-activated protein kinase (AMPK) activation, cells were pre-treated with a 500 μM 5-aminoimidazole-4-carbo xamide-1-β-D-ribofuranoside (AICAR) solution for 12 h and then exposed to 100 mM EtOH for 24 h, following the same treatment schedule used for CA.

Animals. Seven-week-old male C57BL/6 mice (Central Lab. Animal Inc., Korea) were maintained in an air-conditioned room (21-25˚C, 40-60% humidity) with a 12 h light/dark cycle. To investigate the early stages of ALD, particularly hepatic steatosis, liver injury was induced using the chronic-plus-single-binge EtOH feeding model (NIAAA model) as described in a previous study (18). This model was specifically chosen because it more effectively replicates the acute-on-chronic clinical features of human steatosis than traditional chronic feeding models (18). The mice were fed with the Lieber-DeCarli (LDC) diet *ad libitum* for the first 5 days to allow them to adapt to a liquid diet. Subsequently, they were randomly assigned to one of four groups: (1) control, (2) control+CA, (3) EtOH, and (4) CA+EtOH. For 10 days, the EtOH-fed groups were given free access to an LDC diet containing 5% (v/v) EtOH, while the control groups were fed with the standard LDC diet. The mice in the CA-treated group were intraperitoneally (i.p.) injected with 37.5 μg/kg CA once every 2 days. To prepare the injection solution, CA was initially dissolved in DMSO and then diluted to the required concentration in sterile phosphate-buffered saline (PBS). The *in vivo* dose of CA was determined based on its maximum solubility while strictly maintaining the final DMSO concentration below 0.1% (v/v) in the PBS-based vehicle to eliminate any potential vehicle-induced hepatotoxicity. On day 11, the mice were orally administered 5 g/kg of EtOH for the EtOH-fed groups or 9 g/kg of maltose dextrin for the control-fed groups. After 9 h, the mice were sacrificed using CO_2 with a displacement rate of 30% of the chamber volume per minute. The animal experiments were approved by the Chonnam National University Institutional Animal Care and Use Committee (CNU IACUC-YB-2024-123).

Serum chemistry measurement. To obtain mouse serum samples, CO_2 was administrated to anesthetize the mice, and then, their blood was collected via cardiac puncture. The levels of alanine transaminase (ALT) and aspartate transaminase (AST) in the serum were determined using a Catalyst Dx chemistry analyzer (IDEXX Laboratories, Korea).

Histological techniques. Excised livers were fixed in 10% formaldehyde in a phosphate buffer and processed into frozen sections via routine methods. The specimens were sectioned at 4 μm using a cryostat microtome (Leica Biosystems, Nussloch, Germany; CM1950) from the Department of Biological Sciences, College of Natural Sciences, Chonnam National University. The tissues were stained with hematoxylin and eosin (H&E) for histological assessment or 0.5% oil red o solution for the analysis of hepatic lipid accumulation. The stained samples were visualized using a Cytation™ 5 cell imaging multimode reader (BioTek, USA), and quantification analyses were performed using ImageJ software (National Institutes of Health, USA).

MTT assay. An MTT assay was conducted using the MTT reagent (Sigma-Aldrich, USA) to analyze cell viability. Cells were seeded in 96-well plates at a density of $1x10^4$ and cultured for 14-16 h. They were incubated with 0, 50, 100, 500 nM, 1, and 4 μM CA for 24 h. Then, 10 μl of MTT was added to each well, and the plate was incubated at 37˚C for 4 h. The medium was discarded, 100 μl of DMSO was added to each well, and the plate was shaken at 20-25˚C for 15 min. Absorbance was then measured at 550 nm by using a microplate reader (BioTek, USA). The entire MTT assay was performed in the dark.

Quantitative PCR. Total RNA was extracted from cell lysates and mouse tissues using the TRIzol reagent, and cDNA was synthesized from 2 μg of RNA in a total volume of 20 μl using a random primer cocktail and reverse transcriptase (Invitrogen, USA). The primers employed for quantitative PCR were designed using PrimerBank (Table SI), and the specificity of each primer was determined by a BLAST search. Quantitative PCR was performed in 15 μl reaction volumes

using SYBR Green/Rox qPCR Mix (Enzynomics, Korea; cat. no. RT500M). The mRNA expression levels of target genes were normalized relative to β-actin and compared among treatment groups via the ΔΔCt method. The specificity of each reaction was confirmed by melting curve analysis.

Western blot analysis. Proteins were extracted using RIPA buffer (Elabscience, China) containing protease and phosphatase inhibitors (Thermo Scientific, USA), and the extracted proteins were quantified using the Bradford assay. One hundred μg of total proteins were then separated via sodium dodecyl sulfate-polyacrylamide gel electrophoresis and transferred to polyvinylidene fluoride membranes. The membranes were blocked with 5% (v/v) skim milk and then incubated overnight at 4˚C with the primary antibody (diluted at 1:1,000): rabbit anti-phospho-AMPKα (Cell Signaling Technology, USA; cat. no. #2531), rabbit anti-AMPKα (Cell Signaling Technology; cat. no. #2532) or mouse anti-β-actin (Santa Cruz Biotechnology, USA; cat. no. sc-47778). Afterward, they were washed and incubated with either horseradish peroxidase-conjugated goat anti-rabbit IgG secondary antibody (Santa Cruz Biotechnology, USA; cat. no. sc-2357) or m-IgGκ binding protein-horseradish peroxidase (Santa Cruz Biotechnology; cat. no. sc-516102), both diluted at 1:10,000, at room temperature for 1 h. They were washed again, and protein bands were detected using the FUSION SOLO 2X imaging system (Vilber, France). Quantification analyses were performed using ImageJ software.

Oxidative stress assays. To measure malondialdehyde (MDA), an indicator of lipid peroxidation, cells were collected and homogenized in ice-cold PBS. The MDA levels were then determined using a TBARS assay kit (Cayman Chemical, USA) according to the manufacturer's instructions. The resulting MDA values were normalized to the total protein concentration.

To measure hydrogen peroxide (H_2O_2) levels, intracellular H_2O_2 was quantified using a Hydrogen Peroxide Assay kit (Biomax, Republic of Korea) following the manufacturer's protocol. Cells were lysed using the provided assay buffer, and the supernatants were collected for the assay, with H_2O_2 concentrations normalized to the total protein content.

Hepatic triglyceride quantification. Hepatic triglyceride (TG) contents were quantified using a commercial colorimetric assay kit (Biomax) according to the manufacturer's instructions. Liver tissues were homogenized in lysis buffer and centrifuged to remove insoluble debris. The supernatants were collected for the assay, and TG concentrations were normalized to total protein content. Results were expressed as nmol TG/mg protein.

Statistical analyses. Data were statistically analyzed using GraphPad Prism 5 (GraphPad Software, USA). Results are expressed as means ± the standard error of the mean (SEM). The term 'n' indicates independent biological replicates (independent experiments performed on separate occasions). Unless otherwise specified, within each biological replicate, samples were measured in technical duplicates, and the values were averaged to generate a single value per biological replicate. Normality and homogeneity of variance were assessed for each variable prior to statistical testing. To assess statistical significance, unpaired two-tailed Student's t-tests were used for comparisons between two groups, while one-way analyses of variance (ANOVAs) followed by Tukey's post hoc tests were employed for multiple-group comparisons. Significance was accepted at $P<0.05$.

Results

CA reduces ethanol-induced lipid accumulation in hepatocytes. The effect of CA on the cell viability of hepatocytes was assessed. Specifically, the viability of AML12 and Huh7 cells exposed to 50, 100, 500 nM, 1, and 4 μM CA for 24 h was evaluated. Up to 4 μM, CA did not affect cell viability (Fig. 1A). Therefore, 4 μM was selected as the treatment concentration in later assays.

Previous studies have reported that fat accumulation in hepatocytes is induced as an initial liver injury response to EtOH (5,19). Thus, we evaluated the effect of CA on EtOH-induced lipid accumulation in hepatocytes. We found that EtOH treatment induced lipid droplet accumulation, but the CA pre-treatment reduced this accumulation (Fig. 1B). Treatment with CA alone had no effect. Therefore, CA attenuated EtOH-induced lipid accumulation.

CA does not affect lipogenesis but enhances β-oxidation gene expression to attenuate lipid accumulation. EtOH-induced lipid accumulation is induced by increased lipogenesis and/or decreased β-oxidation. To investigate the mechanism by which CA regulates hepatic lipid accumulation, we examined the expression levels of the genes involved in lipogenesis and β-oxidation in human and mouse hepatocytes. The mRNA levels of *SREBP-1c*, *FASN*, and *SCD1* were not significantly altered by CA treatment either alone or in combination with EtOH treatment (Fig. 2A). This result indicates that CA did not suppress EtOH-induced hepatic lipid accumulation by inhibiting lipogenesis. Similarly, the CA treatment did not attenuate EtOH-induced reactive oxygen species (ROS) production, as measured by H_2O_2 and MDA levels (Fig. S1). Therefore, the protective effect of CA was unlikely mediated by oxidative stress reduction.

In contrast, co-treatment with CA and EtOH significantly upregulated the expression of β-oxidation-related genes, including carnitine palmitoyltransferase 1A (*CPT1a*) and *PPARα*, compared with that of EtOH treatment alone (Fig. 2B). These findings show that CA ameliorated EtOH-induced lipid accumulation by promoting fatty acid oxidation. In addition, AICAR, used as a positive control, increased AMPK phosphorylation in EtOH-treated hepatocytes, and CA similarly elevated p-AMPK levels (Fig. S2), supporting involvement of AMPK signaling in CA-induced upregulation of β-oxidation under EtOH exposure.

CA alleviates early EtOH-induced hepatic injury and lipid accumulation in vivo. To evaluate the protective effect of CA against EtOH-induced hepatic steatosis *in vivo*, we assessed the serum levels of liver injury markers. Intraperitoneal administration of CA alone did not significantly alter serum ALT and AST levels compared to those in the control mice,

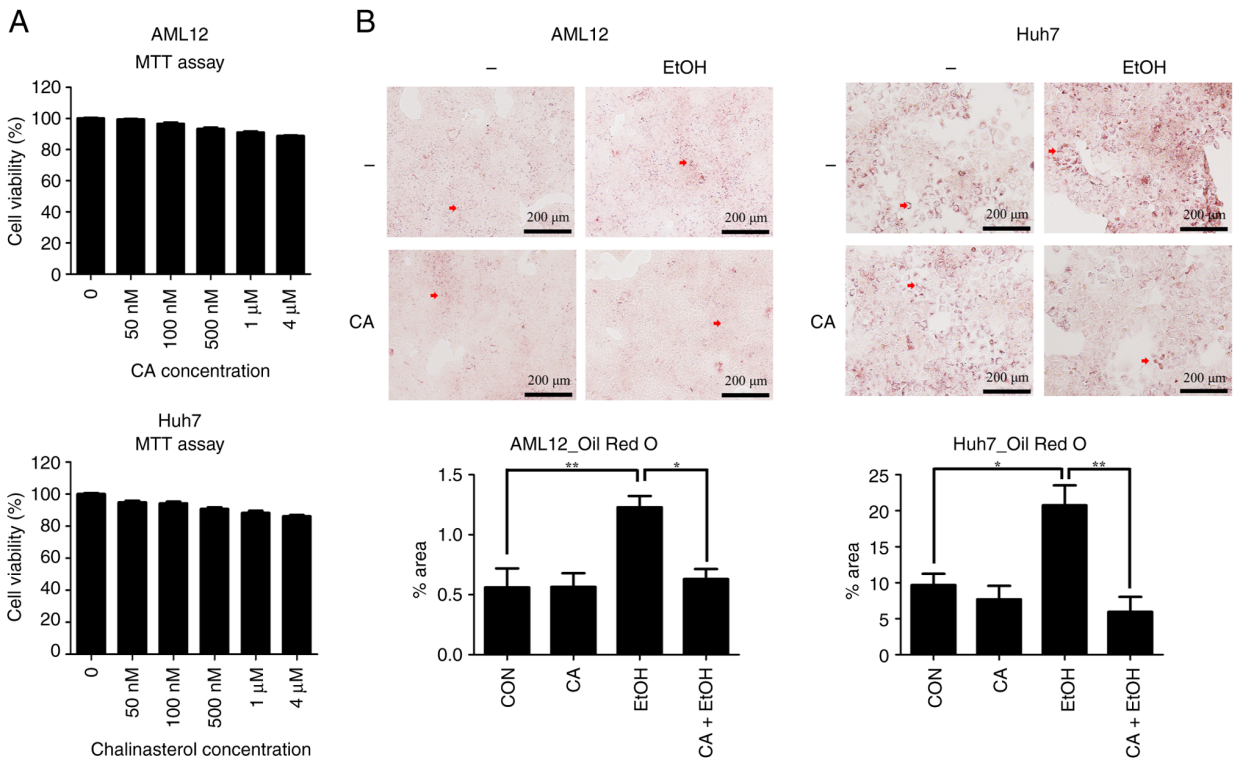

Figure 1. CA reduces EtOH-induced lipid accumulation in hepatocytes. (A) The cell viabilities of AML12 and Huh7 cells treated with 50 nM - 4 μM CA for 24 h. No significant cytotoxicity was observed. (B) Lipid accumulation in AML12 and Huh7 cells treated with 100 mM EtOH for 24 h with or without a 12 h 4 μM CA pre-treatment (scale bars, 200 μm). Red arrows indicate lipid droplets. Data are presented as means ± the SEM. *P<0.05 and **P<0.01. CA, Chalinasterol; EtOH, ethanol; CON, control.

indicating that the selected dose of CA did not induce systemic hepatotoxicity (Fig. 3A). In contrast, EtOH administration significantly increased serum ALT and AST levels, whereas the co-treatment with CA attenuated this increase (Fig. 3A). This suggests that CA mitigates early EtOH-induced liver injury.

While histological analyses revealed no hepatic damage in the EtOH-treated mice (Fig. 3B), EtOH administration caused lipid droplets to accumulate in liver tissues. The CA treatment produced no detectable difference in lipid distribution compared to the control group, but CA administration markedly reduced the EtOH-induced lipid accumulation (Fig. 3C). Consistent with these histological findings, biochemical quantification showed that EtOH increased hepatic TG levels, and the CA co-treatment significantly reduced EtOH-induced TG accumulation (Fig. S3). Collectively, these data indicate that CA attenuate EtOH-induced liver injury and steatosis primarily by suppressing hepatic lipid accumulation.

CA enhances β-oxidation-related gene expression and AMPK activation in vivo. To elucidate the molecular mechanism underlying the protective effect of CA *in vivo*, we examined the expression levels of lipid metabolism-related genes in liver tissues. Consistent with the *in vitro* findings, compared to the control group, CA administration did not significantly affect the expression of lipogenic genes *SREBP-1c*, *FASN*, and *SCD1* (Fig. 4A). Quantitative PCR analyses showed that CA also did not alter the mRNA levels of these lipogenic genes in EtOH-treated mice (Fig. 4A). However, while showing no effect on lipogenesis, the CA treatment significantly upregulated the expression of genes related to fatty acid oxidation. While CA administration alone slightly elevated the mRNA levels of *CPT1a* compared to the control group, a significant upregulation of both *CPT1a* and *PPARα* was seen in the CA+EtOH group when compared to the EtOH group (Fig. 4B). Therefore, CA promoted fatty acid β-oxidation in the liver, particularly under EtOH-induced stress conditions.

Protein analysis revealed the status of AMPK activation. Alone, CA administration showed a tendency to increase p-AMPK levels compared to the control group, but notably, p-AMPK levels were clearly greater in CA+EtOH group mice than in EtOH group mice (Fig. 4C). Thus, CA appears to activate the AMPK pathway, which may contribute to the upregulation of β-oxidation and the attenuation of hepatic EtOH-induced liver injury due to fat accumulation.

Discussion

Alcohol-related liver disease remains a major global health issue, and the earliest and most reversible stage in its progression is alcoholic steatosis (20). Because late-stage ALD has no effective therapy other than liver transplantation (4), treatments targeting hepatic steatosis are critical. In the present study, CA attenuated EtOH-induced hepatic lipid accumulation *in vitro* and *in vivo* primarily by enhancing fatty acid β-oxidation rather than suppressing lipogenesis. These findings suggest that CA may help manage lipid metabolism during the early stages of EtOH exposure.

Previous studies have established that ethanol promotes hepatic steatosis by increasing lipogenesis via SREBP-1

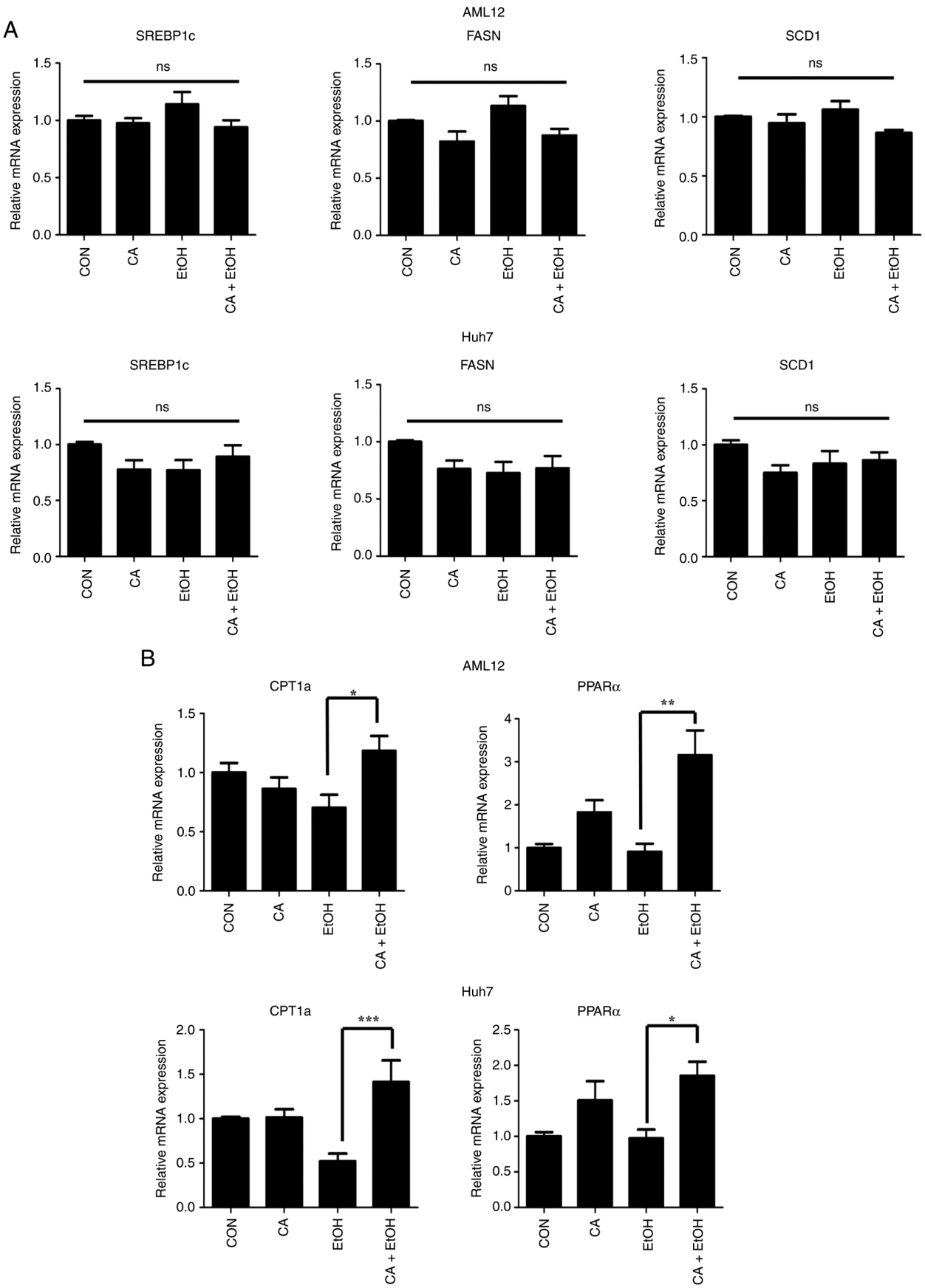

Figure 2. CA enhances β-oxidation, reducing lipid accumulation. (A) The mRNA expression of lipogenesis-related genes *SREBP-1c*, *FASN* and *SCD1* in AML12 and Huh7 cells treated with 100 mM EtOH for 24 h with or without a 12 h 4 μM CA pre-treatment. (B) The mRNA expression of β-oxidation-related genes *CPT1a* and *PPARα* in AML12 and Huh7 cells treated with 100 mM of EtOH for 24 h after 12 h pre-treatment with 4 μM CA. Data are presented as means ± the SEM. *P<0.05, **P<0.01 and ***P<0.001. CA, Chalinasterol; EtOH, ethanol; ns, not significant; CON, control; SREBP-1, sterol regulatory element-binding protein 1; FASN, fatty acid synthase; SCD1, stearoyl-CoA desaturase 1; CPT1A, carnitine palmitoyltransferase 1A; PPARα, peroxisome proliferator-activated receptor α.

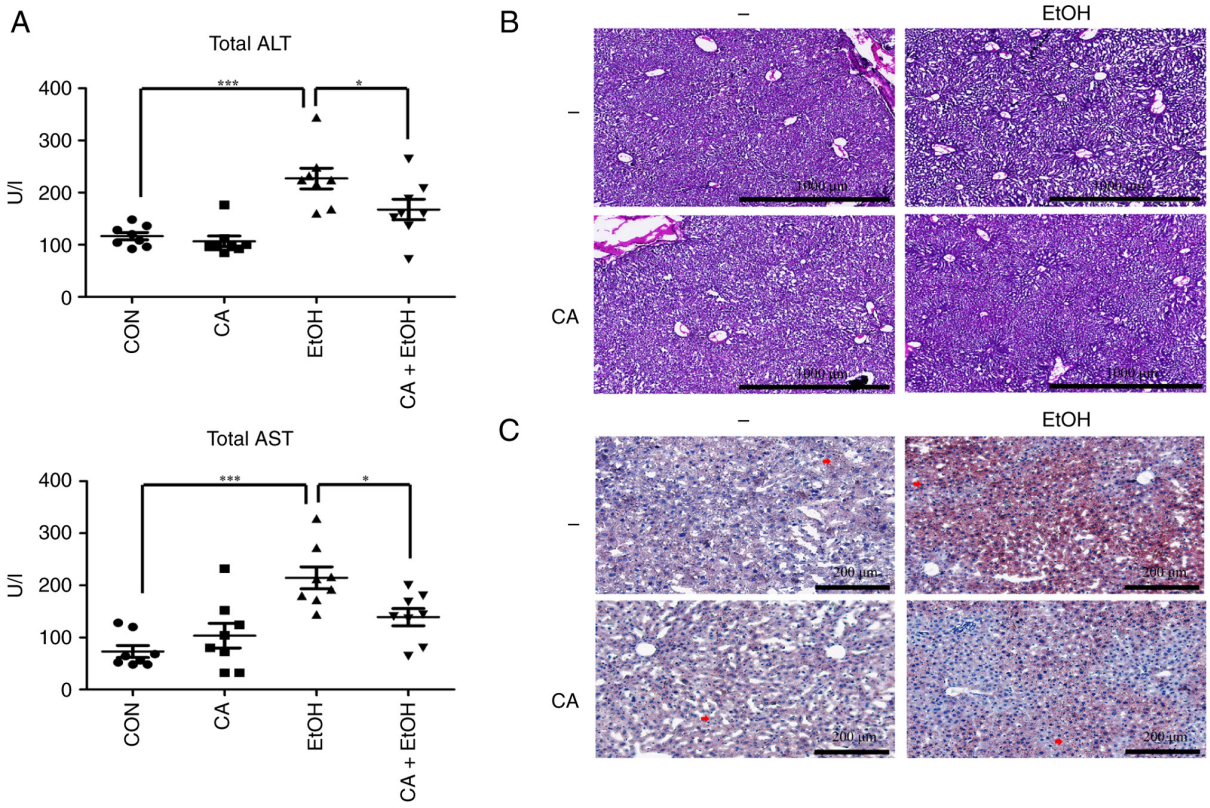

Figure 3. CA attenuates EtOH-induced hepatic steatosis and liver injury *in vivo*. (A) Serum levels of liver injury markers ALT and AST in control and EtOH-fed mice with or without CA administration at 37.5 μg/kg (n=8 per group). (B) Liver sections of control and EtOH-fed mice with or without CA administration at 37.5 μg/kg were stained with H&E (scale bars, 1,000 μm). (C) Lipid droplet accumulation of liver tissues of control and EtOH-fed mice with or without the administration of CA at 37.5 μg/kg (scale bars, 200 μm). Red arrows indicate lipid droplets. Data are presented as means ± the SEM. *P<0.05 and ***P<0.001. CA, Chalinasterol; EtOH, ethanol; ALT, alanine transaminase; AST, aspartate transaminase; H&E, hematoxylin & eosin.

signaling (9) and by impairing lipid oxidation through the suppression of PPARα signaling (10). Consistent with this finding, our results showed that EtOH treatment induced lipid droplet accumulation in hepatocytes and liver tissues. However, the CA pre-treatment did not affect the expression of the lipogenic genes *SREBP-1c*, *FASN*, and *SCD1*; thus, CA did not act by inhibiting EtOH-induced fatty acid synthesis. Furthermore, while oxidative stress is a known driver of ALD, CA treatment did not significantly reduce EtOH-induced ROS production in our cell models. This finding could be attributed to several factors, including the specific ROS targeted or the time point used for detection in our assays. Since EtOH-induced ROS generation occurs in waves, our snapshot measurement might have missed transient antioxidant effects. However, CA may exhibit a regulatory role on lipid metabolism pathways that is distinct from direct antioxidant scavenging. Thus, our results suggest that the protective effect of CA is primarily mediated through metabolic reprogramming rather than a direct reduction of oxidative stress. It significantly upregulated the expression levels of *CPT1a* and *PPARα*, key regulators of fatty acid β-oxidation, in EtOH-treated hepatocytes and the liver tissues of EtOH-fed mice. Additionally, the CA co-treatment significantly increased levels of phosphorylated AMPK, a major regulator of energy metabolism that facilitates lipid catabolism under stress conditions (21). Therefore, CA may activate the AMPK-PPARα axis, promoting fatty acid oxidation and, consequently, reducing lipid accumulation in the liver.

Interestingly, CA-induced AMPK activation is consistent with the mechanism of metformin, a classical AMPK activator widely used for metabolic disorders (22). However, metformin frequently causes gastrointestinal intolerance and although rare, carries a risk of lactic acidosis in susceptible patients (23). As a bioactive dietary compound, CA may have potential as a nutritional adjunct or preventive strategy for early-stage alcoholic steatosis, particularly in settings where long-term tolerability is prioritized. Nevertheless, direct head-to-head comparisons with metformin, to assess efficacy, dose-response patterns, and safety/toxicology profiling, will be required to define its translational value.

Importantly, our *in vivo* data showed that the serum levels of the liver injury markers ALT and AST were increased by EtOH exposure, and this increase was significantly attenuated by CA administration, although histological evidence of liver damage was not observed at the EtOH dose used. Considering that ALT and AST serum levels are used as sensitive early indicators of liver injury (24), even though histological changes were not evident, these altered serum levels suggest that CA has the potential to alleviate early-stage liver damage, highlighting its potential role in supporting liver health during early EtOH-induced stress.

Our findings are consistent with previous reports, which showed that natural compounds can modulate hepatic lipid metabolism via AMPK and PPARα pathways. Various natural chemicals, including total saponins from *Panax japonicas* (25) and gallic acid (26) weaken lipid accumulation in hepatocytes

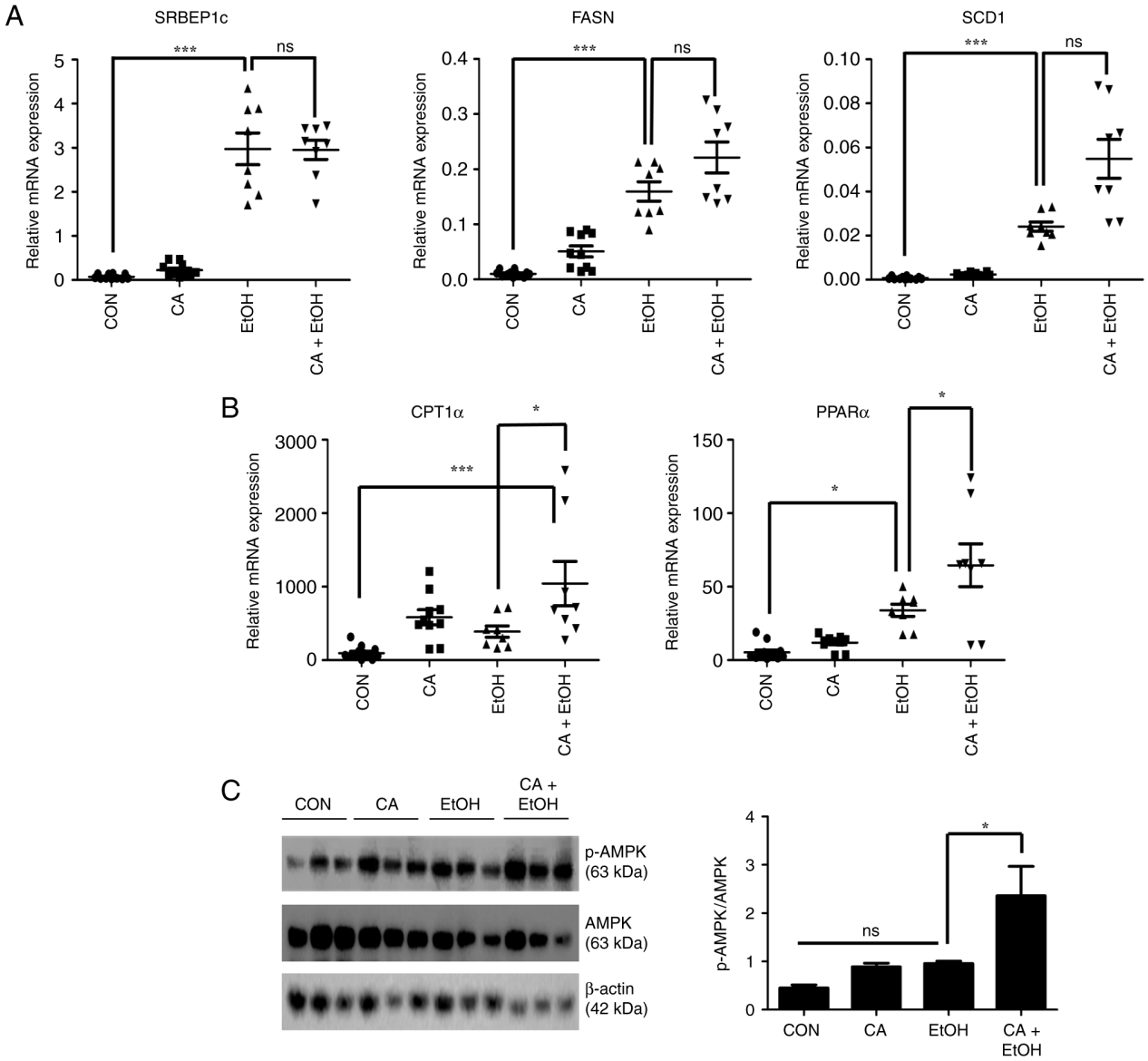

Figure 4. CA enhances β-oxidation-related gene expression and activates AMPK signaling *in vivo*. (A) The relative mRNA expression levels of lipogenesis-related genes *SREBP-1c*, *FASN*, and *SCD1* in liver tissues of ethanol (EtOH)-treated mice with or without CA administration at 37.5 μg/kg, determined using quantitative PCR (n=8 per group). (B) The relative mRNA expression levels of β-oxidation-related genes *CPT1a* and *PPARα* in liver tissues of EtOH-treated mice with or without CA administration at 37.5 μg/kg (n=8 per group). (C) Protein levels of phosphorylated AMPK and AMPK in liver tissues of control and EtOH-fed mice with or without CA administration at 37.5 μg/kg. Data are presented as means ± the SEM. *P<0.05, and ***P<0.001. CA, Chalinasterol; AMPK, AMP-activated protein kinase; CPT1A, carnitine palmitoyltransferase 1A; EtOH, ethanol; FASN, fatty acid synthase; PPARα, peroxisome proliferator-activated receptor α; SCD1, stearoyl-CoA desaturase 1; SREBP-1, sterol regulatory element-binding protein 1; ns, not significant.

by activating AMPK signaling and promoting fatty acid oxidation. These studies support the potential of natural compounds as therapeutic agents in lipid metabolism disorders. Therefore, CA promotes fatty acid oxidation and reduces EtOH-induced fat accumulation. Consequently, lipid metabolism in the liver is restored, showing that CA is a potential candidate for further studies related to alcohol-associated liver injury.

Nonetheless, this study has several limitations. Only the early-stage effects of CA were evaluated, and its long-term effects on fibrosis or cirrhosis were not characterized. Further studies using chronic ALD models will be required to evaluate CA's efficacy against steatohepatitis and fibrosis. Furthermore, while our study focused on the downstream effects of CA on lipid metabolism, we cannot entirely rule out the possibility that CA indirectly influences hepatic steatosis by modulating EtOH-metabolizing enzymes, such as alcohol dehydrogenase or aldehyde dehydrogenase. Further research should investigate whether CA affects the rate of EtOH metabolism to fully elucidate its protective mechanisms. Moreover, although AMPK was activated, we did not directly confirm the link between AMPK signaling and downstream gene regulation through inhibitor or knockout approaches. Future studies involving AMPK or PPARα loss-of-function models should be employed to validate the proposed mechanism. Lastly, the pharmacokinetic properties and bioavailability of CA were not assessed. Although effective concentrations were used *in vitro* and *in vivo* in this study, the mechanism through which CA is absorbed, metabolized, and distributed in the body remains unclear. This information is crucial for devising dosing strategies and determining clinical potential. Despite

these limitations, our study provides important insights into the early intervention potential of CA in EtOH-induced lipid accumulation and a basis for performing future mechanistic and translational investigations.

In conclusion, our study provides evidence that CA reduces EtOH-induced hepatic lipid accumulation and early liver injury by enhancing β-oxidation through AMPK-PPARα pathway activation. Given the global burden of ALD and the lack of effective treatments for advanced stages, CA represents a potential candidate for early preventive interventions aimed at mitigating alcoholic steatosis.

Acknowledgements

Not applicable.

Funding

This work was supported by the National Research Foundation of Korea (grant no. RS-2023-00251463) and Chonnam National University (grant no. 2024-1145-01).

Availability of data and materials

The data generated in the present study may be requested from the corresponding author.

Authors' contributions

JHK conceptualized and designed this study, collected, assembled and analyzed data, and wrote the manuscript. MYK collected, assembled and analyzed data. SO conceptualized and designed this study. DHL conceptualized and designed this study, collected, assembled, analyzed and interpreted data, wrote the manuscript, and provided financial support. JHK and DHL confirm the authenticity of all the raw data. All authors have read and approved the final manuscript.

Ethics approval and consent to participate

The animal experiments were approved by the Chonnam National University Institutional Animal Care and Use Committee (approval no. CNU IACUC-YB-2024-123).

Patient consent for publication

Not applicable.

Competing interests

The authors declare that they have no competing interests.

References

1. World Health Organization: Global status report on alcohol and health 2018. World Health Organization, Geneva, 2018.
2. Rehm J, Baliunas D, Borges GL, Graham K, Irving H, Kehoe T, Parry CD, Patra J, Popova S, Poznyak V, *et al*: The relation between different dimensions of alcohol consumption and burden of disease: An overview. Addiction 105: 817-843, 2010.
3. Ohashi K, Pimienta M and Seki E: Alcoholic liver disease: A current molecular and clinical perspective. Liver Res 2: 161-172, 2018.
4. Schuppan D and Afdhal NH: Liver cirrhosis. Lancet 371: 838-851, 2008.
5. Gao B and Bataller R: Alcoholic liver disease: Pathogenesis and new therapeutic targets. Gastroenterology 141: 1572-1585, 2011.
6. Lieber CS: Effects of ethanol upon lipid metabolism. Lipids 9: 103-116, 1974.
7. You M and Arteel GE: Effect of ethanol on lipid metabolism. J Hepatol 70: 237-248, 2019.
8. Horton JD, Goldstein JL and Brown MS: SREBPs: Activators of the complete program of cholesterol and fatty acid synthesis in the liver. J Clin Invest 109: 1125-1131, 2002.
9. You M and Crabb DW: Recent advances in alcoholic liver disease II. Minireview: Molecular mechanisms of alcoholic fatty liver. Am J Physiol Gastrointest Liver Physiol 287: G1-G6, 2004.
10. Galli A, Pinaire J, Fischer M, Dorris R and Crabb DW: The transcriptional and DNA binding activity of peroxisome proliferator-activated receptor alpha is inhibited by ethanol metabolism: A novel mechanism for the development of ethanol-induced fatty liver. J Biol Chem 276: 68-75, 2001.
11. Menaa F, Wijesinghe U, Thiripuranathar G, Althobaiti NA, Albalawi AE, Khan BA and Menaa B: Marine algae-derived bioactive compounds: A new wave of nanodrugs? Mar Drugs 19: 484, 2021.
12. Yun MY, Lee JS, Kim BS and Choi HJ: Capsosiphon fulvescens extracts improve obesity-associated metabolic disorders and hepatic steatosis in high-fat diet-induced obese mice. Anim Sci J 89: 589-596, 2018.
13. de Almeida CL, Falcão Hde S, Lima GR, Montenegro Cde A, Lira NS, de Athayde-Filho PF, Rodrigues LC, de Souza Mde F, Barbosa-Filho JM and Batista LM: Bioactivities from marine algae of the genus Gracilaria. Int J Mol Sci 12: 4550-4573, 2011.
14. Fernando IS, Nah JW and Jeon YJ: Potential anti-inflammatory natural products from marine algae. Environ Toxicol Pharmacol 48: 22-30, 2016.
15. Wan-Loy C and Siew-Moi P: Marine algae as a potential source for anti-obesity agents. Mar Drugs 14: 222, 2016.
16. Kwon MJ and Nam TJ: Effects of mesangi (Capsosiphon fulvecens) powder on lipid metabolism in high cholesterol fed rats. J Korean Soc Food Sci Nutr 35: 530-535, 2006.
17. Islam MN, Choi SH, Moon HE, Park JJ, Jung HA, Woo MH, Woo HC and Choi JS: The inhibitory activities of the edible green alga Capsosiphon fulvescens on rat lens aldose reductase and advanced glycation end products formation. Eur J Nutr 53: 233-242, 2014.
18. Bertola A, Mathews S, Ki SH, Wang H and Gao B: Mouse model of chronic and binge ethanol feeding (the NIAAA model). Nat Protoc 8: 627-637, 2013.
19. Tsukamoto H, Machida K, Dynnyk A and Mkrtchyan H: 'Second hit' models of alcoholic liver disease. Semin Liver Dis 29: 178-187, 2009.
20. O'shea RS, Dasarathy S and McCullough AJ; Practice Guideline Committee of the American Association for the Study of Liver Diseases; Practice Parameters Committee of the American College of Gastroenterology: Alcoholic liver disease. Hepatology 51: 307-328, 2010.
21. Hardie DG: AMP-activated/SNF1 protein kinases: Conserved guardians of cellular energy. Nat Rev Mol Cell Biol 8: 774-785, 2007.
22. Viollet B, Guigas B, Sanz Garcia N, Leclerc J, Foretz M and Andreelli F: Cellular and molecular mechanisms of metformin: An overview. Clin Sci (Lond) 122: 253-270, 2011.
23. Mazumder A, Singh A and Sujeet JHA: A Review on metformin: Clinical significance and side effects. Int J Pharm Res 13: 60, 2021.
24. Louvet A and Mathurin P: Alcoholic liver disease: Mechanisms of injury and targeted treatment. Nat Rev Gastroenterol Hepatol 12: 231-242, 2015.
25. Qiu L, Feng R, Wu QS, Wan JB and Zhang QW: Total saponins from Panax japonicus attenuate acute alcoholic liver oxidative stress and hepatosteatosis by p62-related Nrf2 pathway and AMPK-ACC/PPARα axis in vivo and in vitro. J Ethnopharmacol 317: 116785, 2023.
26. Zhang J, Zhang W, Yang L, Zhao W, Liu Z, Wang E and Wang J: Phytochemical gallic acid alleviates nonalcoholic fatty liver disease via AMPK-ACC-PPARa axis through dual regulation of lipid metabolism and mitochondrial function. Phytomedicine 109: 154589, 2023.